

See discussions, stats, and author profiles for this publication at: <https://www.researchgate.net/publication/231630156>

# Surface characterization of Ga<sub>2</sub>O<sub>3</sub>-TiO<sub>2</sub> and V<sub>2</sub>O<sub>5</sub>/Ga<sub>2</sub>O<sub>3</sub>-TiO<sub>2</sub> catalysts

ARTICLE · JUNE 2001

DOI: 10.1021/jp010763o

CITATIONS

43

READS

15

5 AUTHORS, INCLUDING:



**Benjaram M Reddy**

CSIR-Indian Institute of Chemical Technology

279 PUBLICATIONS 5,376 CITATIONS

SEE PROFILE



**Ganesh Ibram**

International Advanced Research Centre for ...

74 PUBLICATIONS 1,456 CITATIONS

SEE PROFILE



**Asuncion Fernandez**

Spanish National Research Council - Institut...

244 PUBLICATIONS 6,277 CITATIONS

SEE PROFILE



**Panagiotis G Smirniotis**

University of Cincinnati

146 PUBLICATIONS 5,117 CITATIONS

SEE PROFILE

Article

## Surface Characterization of GaO–TiO and VO/GaO–TiO Catalysts

Benjaram M. Reddy, Ibram Ganesh, Ettireddy P. Reddy, Asuncin Fernndez, and Panagiotis G. Smirniotis

*J. Phys. Chem. B*, **2001**, 105 (26), 6227-6235 • DOI: 10.1021/jp010763o • Publication Date (Web): 05 June 2001

Downloaded from <http://pubs.acs.org> on April 27, 2009

### More About This Article

Additional resources and features associated with this article are available within the HTML version:

- Supporting Information
- Links to the 1 articles that cite this article, as of the time of this article download
- Access to high resolution figures
- Links to articles and content related to this article
- Copyright permission to reproduce figures and/or text from this article

[View the Full Text HTML](#)



ACS Publications  
High quality. High impact.

Surface Characterization of  $\text{Ga}_2\text{O}_3\text{--TiO}_2$  and  $\text{V}_2\text{O}_5/\text{Ga}_2\text{O}_3\text{--TiO}_2$  Catalysts

Benjaram M. Reddy,<sup>\*,†</sup> Ibram Ganesh,<sup>†</sup> Ettireddy P. Reddy,<sup>†,‡,§</sup> Asunción Fernández,<sup>‡</sup> and Panagiotis G. Smirniotis<sup>\*,§</sup>

*Inorganic and Physical Chemistry Division, Indian Institute of Chemical Technology, Hyderabad 500 007, India, Centro de Investigaciones Científicas, Instituto de Ciencia de Materiales de Sevilla, Isla de la Cartuja, Avda. Américo Vespucio s/n, 41092 Sevilla, Spain, and Chemical Engineering Department, University of Cincinnati, Ohio 45221-0171*

*Received: February 28, 2001; In Final Form: May 1, 2001*

The techniques of X-ray photoelectron spectroscopy, X-ray diffraction, FT-infrared, and  $\text{O}_2$  chemisorption were employed to characterize a specially obtained  $\text{Ga}_2\text{O}_3\text{--TiO}_2$  mixed oxide and  $\text{V}_2\text{O}_5/\text{Ga}_2\text{O}_3\text{--TiO}_2$  catalyst calcined at different temperatures from 773 to 1073 K. The  $\text{Ga}_2\text{O}_3\text{--TiO}_2$  (1:5 mole ratio based on the oxides) mixed oxide was synthesized by a homogeneous coprecipitation method with in situ generated ammonium hydroxide, and a nominal 4 wt %  $\text{V}_2\text{O}_5$  was impregnated over the calcined support (773 K) by adopting a wet impregnation technique. A commercial  $\text{TiO}_2$  (anatase) sample was also used in this study for comparison purposes. The characterization results suggest that the  $\text{Ga}_2\text{O}_3\text{--TiO}_2$  mixed oxide, calcined at 773 K, primarily consists of a mixture of  $\text{TiO}_2$  anatase and  $\alpha\text{-Ga}_2\text{O}_3$ . In the case of the  $\text{V}_2\text{O}_5/\text{Ga}_2\text{O}_3\text{--TiO}_2$  catalyst, the impregnated  $\text{V}_2\text{O}_5$  is in a highly dispersed state on the surface of the mixed oxide. Under the influence of thermal treatments from 773 to 1073 K, the dispersed vanadium oxide promotes the transformation of anatase to rutile and  $\alpha\text{-Ga}_2\text{O}_3$  to  $\beta\text{-Ga}_2\text{O}_3$  and is accompanied by a loss in the specific surface area of the samples. In particular, the gallia in the  $\text{V}_2\text{O}_5/\text{Ga}_2\text{O}_3\text{--TiO}_2$  catalyst retards the transformation of anatase into rutile. The Ti 2p, Ga 3d, and V 2p photoelectron peaks of the  $\text{V}_2\text{O}_5/\text{Ga}_2\text{O}_3\text{--TiO}_2$  sample are highly sensitive to the calcination temperature. The intensity of the Ti 2p line increased with increasing calcination temperature and an opposite trend was noted in the case of Ga 3d and V 2p lines. The XPS line shapes and the corresponding binding energies indicate that the dispersed vanadium oxide in the  $\text{V}_2\text{O}_5/\text{Ga}_2\text{O}_3\text{--TiO}_2$  catalyst interacts preferably with the gallium oxide. The V/Ti and V/Ga atomic ratios as determined by XPS measurements reveal that more vanadium is confined to Ti than Ga at 773 and 873 K and almost equally at 973 and 1073 K calcination temperatures, respectively.

## Introduction

Titania (anatase) has been widely employed as a support as well as catalyst for a variety of applications.<sup>1–4</sup> In particular, the  $\text{TiO}_2$  anatase has been extensively used for several photocatalytic reactions for the elimination of many organic pollutants from wastewaters.<sup>4</sup> Titania-based catalysts are also employed for HCN and COS hydrolysis and silica-supported titania for olefin epoxidations.<sup>5</sup> The influence of several transition-metal species on the photocatalytic/catalytic activity of pure  $\text{TiO}_2$  for various reactions has also been the object of some recent investigations for improving the efficiency of these processes.<sup>4,6–8</sup> However, great disadvantages associated with  $\text{TiO}_2$  are its low specific surface area, poor mechanical strength, and lack of abrasion resistance. In addition, the titania anatase has poor thermal stability at high temperatures. The thermal stability of a catalyst is one of the very important factors in catalyst selection, since in high-temperature oxidations or selective catalytic reduction (SCR), long-term thermal stability dictates the catalyst life. Therefore, there are few attempts in the

literature to overcome all the deficiencies of the titania in view of its commercial importance.<sup>9–13</sup>

The proximity of gallium to zinc in the periodic table would suggest its efficacy as a promoter. The possibility of gallium substitution for alumina in zeolite structure has been known for some time. Gallium impregnated on a high surface area silica has been reported to be an effective dehydrocyclodimerization catalyst capable of catalyzing the conversion of isobutene or isobutane into xylenes.<sup>14</sup> Gallium oxide alone was also employed as an active catalyst for dehydrogenation of ethane to ethene in the presence of carbon dioxide.<sup>15</sup> The Ga-containing zeolites for light paraffin aromatization have received considerable interest since their incorporation in the Cyclar process.<sup>16</sup> Many different formulas of Ga/HZSM-5 have been reported to be useful for paraffin aromatization, including the catalysts prepared by ion exchange<sup>17</sup> or impregnation<sup>18</sup> of gallium salts on ZSM-5, gallosilicates,<sup>19</sup> and mechanical mixtures of  $\text{Ga}_2\text{O}_3$  with ZSM-5.<sup>20</sup> The gallium-promoted  $\text{TiO}_2$  mixed oxide after impregnating with  $\text{V}_2\text{O}_5$  was found to exhibit better catalytic properties for the selective oxidation of 4-methylanisole to anisaldehyde, recently.<sup>21</sup> Anisaldehyde is an important chemical intermediate in the perfumery, pharmaceutical, and agrochemical intermediates. In particular, the  $\text{V}_2\text{O}_5/\text{Ga}_2\text{O}_3\text{--TiO}_2$  combination catalyst provided a maximum conversion of 72% with 90% anisaldehyde product selectivity.<sup>21</sup> Very interestingly, the same combination

\* To whom correspondence should be addressed. For B.M.R.: fax, (91) 40 7173387; e-mail, bmreddy@iict.ap.nic.in. For P.G.S.: fax, (513) 556-3473; e-mail, panagiotis.smirniotis@uc.edu.

<sup>†</sup> Indian Institute of Chemical Technology.

<sup>‡</sup> Instituto de Ciencia de Materiales de Sevilla.

<sup>§</sup> University of Cincinnati.

catalyst was also found to exhibit very promising catalytic properties for the one-step synthesis of 2,6-dimethylphenol from methanol and cyclohexanone mixtures.<sup>22</sup> The 2,6-dimethylphenol is an important chemical intermediate in the polymer industry for engineering plastics. Synthesis of 2,6-dimethylphenol from methanol and cyclohexanone mixtures is a complex reaction of oxidative dehydrogenation and alkylation in a single step. The  $\text{V}_2\text{O}_5/\text{Ga}_2\text{O}_3\text{--TiO}_2$  mixed oxide catalyst possesses a combination of acid–base and redox properties together, thus, exhibiting very interesting catalytic activity. The  $\text{Ga}_2\text{O}_3\text{--TiO}_2$  composite oxide was also reported to be an interesting material having numerous applications in the areas of photocatalysis, electrocatalysis, and materials science.<sup>23,24</sup> In view of their significance, a comprehensive investigation was undertaken to fully understand the genesis of these materials.

The primary objective of this investigation, in particular, was to follow the structural evaluation of  $\text{Ga}_2\text{O}_3\text{--TiO}_2$  mixed oxide and the dispersion and nature of vanadium oxide on this support under the influence of thermal treatments. In the present study, a  $\text{Ga}_2\text{O}_3\text{--TiO}_2$  mixed oxide was obtained by a homogeneous coprecipitation method and was deposited with 4 wt %  $\text{V}_2\text{O}_5$  from ammonium metavanadate by a wet impregnation technique. The  $\text{Ga}_2\text{O}_3\text{--TiO}_2$  mixed oxide and the  $\text{V}_2\text{O}_5/\text{Ga}_2\text{O}_3\text{--TiO}_2$  catalyst were subjected to thermal treatments from 773 to 1073 K and were examined by XPS, XRD, FTIR, BET surface area,  $\text{O}_2$  chemisorption, and other techniques. For comparison purposes, a commercial  $\text{TiO}_2$  (anatase) support was also used in this study.

## Experimental Section

**Catalyst Preparation.** The gallia–titania (1:5 mole ratio) mixed oxide was prepared by a homogeneous coprecipitation method with in situ generated ammonia by decomposition of urea at 368 K.<sup>25</sup> In a typical experiment, the requisite quantities of titanium tetrachloride (Fluka, AR grade) and gallium chloride (obtained by dissolving  $\text{Ga}_2\text{O}_3$  in a hot concentrated HCl solution) were mixed together ( $\text{pH} = 2$ ), to which an excess amount of solid urea was also added (1:2.5 metal to urea molar ratio). The resulting mixture was heated slowly to 363–368 K on a hot plate with vigorous stirring. The pH of the solution was monitored at different intervals of time. No change in the pH of the solution was observed until the temperature reached to 395 K. In about 6 h of heating, as decomposition of urea progressed to a certain extent, the formation of precipitate gradually occurred and the pH of the solution increased to 7–8. To make sure total precipitation of the constituent metals, the pH of the solution was increased to 10 by adding dilute ammonia solution. The precipitate was heated 6 h more to facilitate aging. Thus, formed precipitate was filtered off, washed several times with deionized water until free from chloride ions, and dried at 393 K for 16 h. The obtained sample was calcined at 773 K for 6 h in air atmosphere. Some portions of this finished  $\text{Ga}_2\text{O}_3\text{--TiO}_2$  was once again heated at 873, 973, and 1073 K for 6 h in a closed electrical furnace in air atmosphere.

The  $\text{V}_2\text{O}_5/\text{Ga}_2\text{O}_3\text{--TiO}_2$  catalyst, containing 4 wt %  $\text{V}_2\text{O}_5$  was prepared by a standard wet impregnation method from ammonium metavanadate (Fluka, AR grade) dissolved in aqueous oxalic acid (1 M) solution. After evaporation of excess water on a water bath, the resultant solid was dried at 383 K for 12 h and calcined at 773 K for 5 h in a flow of oxygen. Some portions of the finished catalyst were once again heated at 873, 973, and 1073 K for 6 h in air atmosphere.

For the purpose of comparison, a commercial titanium oxide ( $\text{TiO}_2$ , anatase; May & Baker, England, AR grade) was also

impregnated with 4 wt %  $\text{V}_2\text{O}_5$  from ammonium metavanadate and calcined at 773 K, following the identical procedure described above. Some portions of this finished catalyst and the  $\text{TiO}_2$  alone were also once again treated at 873, 973, and 1073 K for 6 h in a closed electrical furnace in air atmosphere.

**X-ray Diffraction.** X-ray powder diffraction patterns have been recorded on a Siemens D-5000 diffractometer using a  $\text{Cu K}\alpha$  radiation source and a scintillation counter detector. The XRD phases present in the samples were identified with the help of JCPDS data files. For comparison purposes, the fraction of rutile in the catalyst was estimated by using the following equation:

$$X_{\text{R}} = (1 + 0.794I_{\text{a}}/I_{\text{r}})^{-1}$$

where  $I_{\text{a}}$  and  $I_{\text{r}}$  are the intensities of (101) and (110) reflections for anatase and rutile, respectively.<sup>11</sup> The X-ray line broadening technique was used to determine the crystallite size of anatase and rutile in the samples from XRD data of anatase (101) and rutile (110) reflections, which were stored in a computer.<sup>26</sup>

**Infrared Spectra.** The FTIR spectra were recorded on a Nicolet 740 FTIR spectrometer at ambient conditions, using KBr disks, with a nominal resolution of  $4\text{ cm}^{-1}$  and averaging 100 spectra.

**Chemisorption Measurements.** Oxygen uptake measurements, at 643 K by a volumetric method, were conducted on a standard static volumetric high vacuum ( $1 \times 10^{-6}$  Torr) system having the facility for reducing the samples in situ by flowing purified hydrogen ( $35\text{ cm}^3/\text{min}$ ). More details of this method are described elsewhere.<sup>27</sup> After the chemisorption experiment the BET surface area of the sample was determined by  $\text{N}_2$  physisorption at 77 K.

**X-ray Photoelectron Spectroscopy.** XPS spectra were recorded by using a VG-ESCA lab 210 spectrometer working in the constant analyzer energy mode with a pass energy of 50 eV and Mg  $\text{K}\alpha$  radiation as the excitation source. Before experiments the spectrometer was calibrated against  $E_{\text{b}}(\text{Au } 4f_{7/2}) = 84.0\text{ eV}$  and  $E_{\text{b}}(\text{Cu } 2p_{3/2}) = 932.6\text{ eV}$ .<sup>28</sup> The Ti  $2p_{3/2}$  or C 1s lines were taken as internal references with a binding energy of 458.5 and 284.8 eV, respectively.<sup>28</sup> An estimated error of  $\pm 0.1\text{ eV}$  can be assumed for all the measurements. The finely ground oven-dried samples were mounted on the standard sample holder, which can house four samples at a time. The sample holder was fixed on a rod attached to the pretreatment chamber. Before transferring them to the main chamber the samples were degassed ( $1 \times 10^{-7}$  Torr) in the pretreatment chamber overnight at room temperature. The degassed samples were then transferred into the main chamber and the XPS analysis was done at room temperature and pressures typically on the order of  $10^{-10}$  Torr. Quantitative analysis of atomic ratios was accomplished by determining the elemental peak areas, following a Shirley background subtraction by the usual procedures, and carried out using the sensitivity factors supplied with the instrument.<sup>28–30</sup> The modified Auger parameters of Ti and Ga were also calculated according to the well-established procedures in the literature.<sup>28</sup> The Auger parameter is expected to provide valuable information about the electronic properties of the oxides dispersed on metal or metal oxide supports.<sup>31</sup>

**Thermal Analysis.** The DTA–TGA curves were obtained on a Mettler Toledo TG-SDTA apparatus. The sample was heated from ambient temperature to 1273 K under nitrogen flow. The sample weight was ca. 15 mg, and the heating rate was 10 K/min.

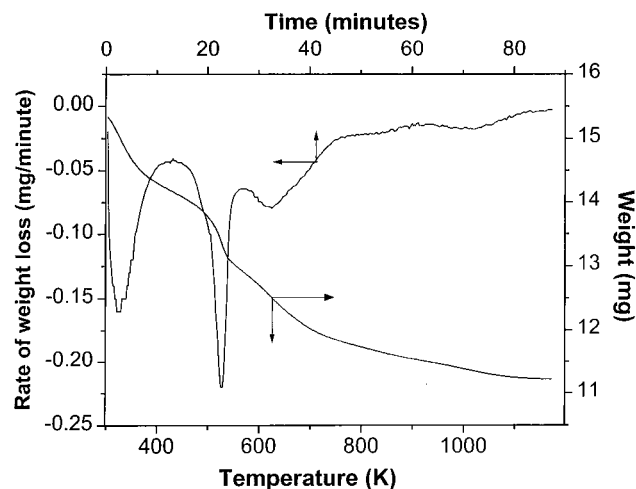


Figure 1. TGA and DTA profile of the uncalcined  $\text{Ga}_2\text{O}_3\text{--TiO}_2$  sample.

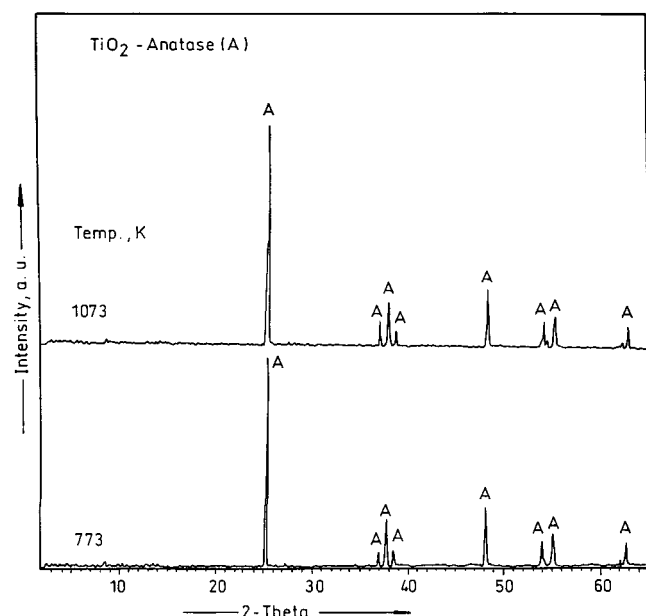


Figure 2. X-ray powder diffraction patterns of  $\text{TiO}_2$  calcined at different temperatures: (A) lines due to anatase.

## Results and Discussion

The coprecipitated  $\text{Ga}_2\text{O}_3\text{--TiO}_2$  mixed oxide was subjected to DTA-TGA analysis before calcination. The obtained thermogram, between 309 and 1173 K at a ramp of 10 K/min, is shown in Figure 1. According to this figure, the gallia-titania mixed oxide obtained by the homogeneous coprecipitation method exhibits two major weight loss peaks. The low-temperature peak in the range 323–388 K is primarily due to loss of nondissociative adsorbed water as well as water held on the surface by hydrogen bonding. A rapid loss of water occurs around 498–648 K due to dehydroxylation of the surface. The loss of sample weight between ambient and 773 K is about 23%; however, the weight loss between 773 and 1173 K is only 3%. It indicates that over the temperature range between 773 and 1173 K, the  $\text{Ga}_2\text{O}_3\text{--TiO}_2$  mixed oxide material is not undergoing any major changes and is quite stable in terms of phases and chemical composition.

A commercial  $\text{TiO}_2$  (anatase, BET SA  $10 \text{ m}^2 \text{ g}^{-1}$ ) was also used in this investigation for comparison purposes. The X-ray powder diffraction patterns of this sample calcined at 773 and 1073 K are shown in Figure 2, which indicate clearly that the

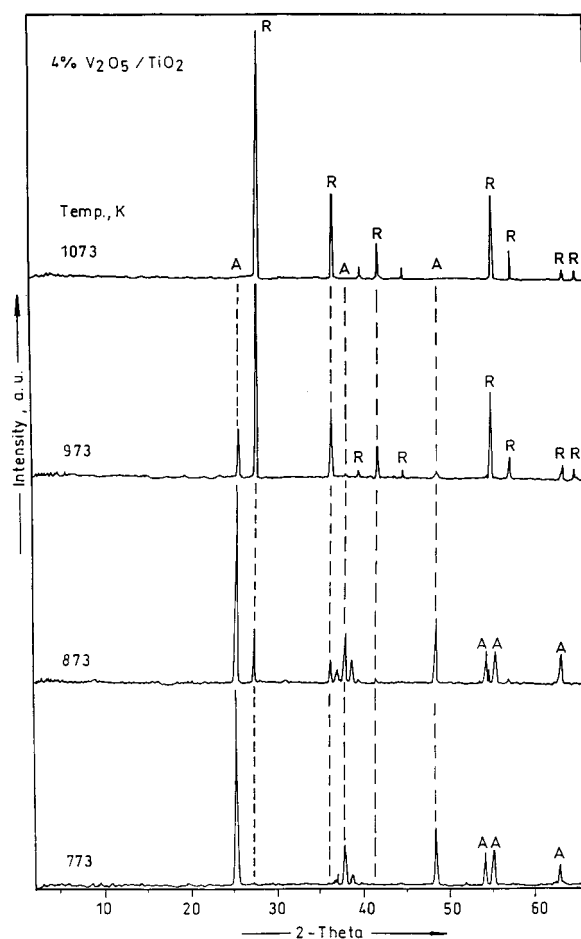
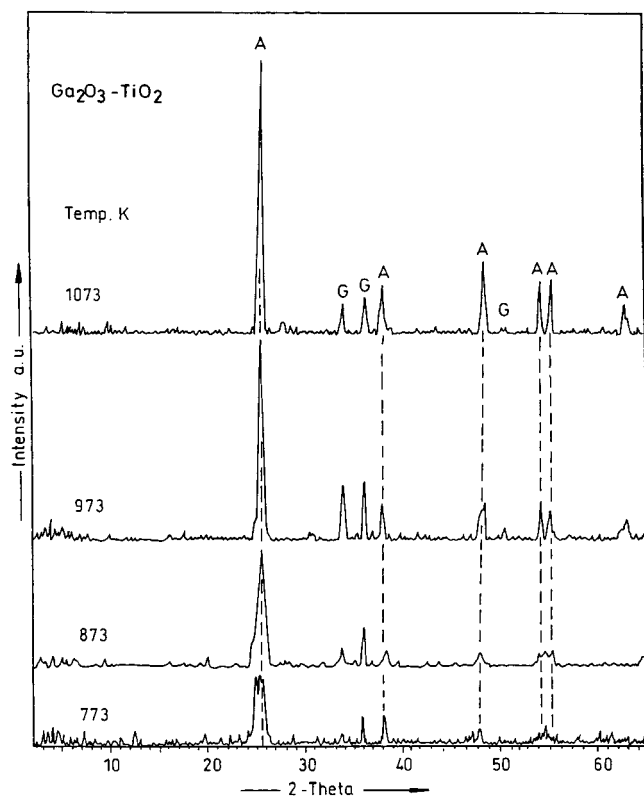


Figure 3. X-ray powder diffraction patterns of 4%  $\text{V}_2\text{O}_5/\text{TiO}_2$  calcined at different temperatures: (A) lines due to anatase; (R) lines due to rutile.

used  $\text{TiO}_2$  sample is in the crystalline anatase form. With increasing calcination temperature from 773 to 1073 K an increase in the intensity of lines can be noted due to further improvement in the crystallinity of the anatase. Most importantly, no lines due to rutile phase are noted even at 1073 K calcination temperature. This observation reveals that the  $\text{TiO}_2$  anatase structure is quite stable up to 1073 K in the absence of any additives to the sample. The XRD profiles of the 4 wt %  $\text{V}_2\text{O}_5/\text{TiO}_2$  catalyst calcined at different temperatures from 773 to 1073 K are shown in Figure 3. A gradual transformation of anatase into rutile phase with increasing calcination temperature can be noted from this figure. The  $\text{TiO}_2$  is in the form of anatase at 773 K, while at 1073 K it is in the rutile state. A closer look at the XRD patterns of  $\text{TiO}_2$  and  $\text{V}_2\text{O}_5/\text{TiO}_2$  samples calcined at various temperatures (Figures 2 and 3) reveals that there are at least two principal differences in their spectra. The first one is that there is a total transformation of anatase into rutile in the case of the  $\text{V}_2\text{O}_5/\text{TiO}_2$  sample, whereas the pure  $\text{TiO}_2$  anatase is quite stable up to 1073 K. The second observation is that there are no lines due to crystalline  $\text{V}_2\text{O}_5$  or a compound between  $\text{V}_2\text{O}_5$  and  $\text{TiO}_2$  even up to 1073 K.

The XRD patterns of  $\text{Ga}_2\text{O}_3\text{--TiO}_2$  mixed oxide calcined at various temperatures from 773 to 1073 K is shown in Figure 4. As can be noted from this figure, the gallia-titania mixed oxide obtained via a homogeneous coprecipitation method and calcined at 773 K exhibits a poor crystallinity. Only the broad diffraction peaks due to  $\text{TiO}_2$  anatase and gallium oxide ( $\alpha\text{-Ga}_2\text{O}_3$ , JCPDS File No. 6-503) can be seen from this figure. With increasing calcination temperature from 773 to 1073 K, a





**Figure 4.** X-ray powder diffraction patterns of  $\text{Ga}_2\text{O}_3\text{-TiO}_2$  calcined at different temperatures: (A) lines due to anatase; (G) lines due to  $\alpha\text{-Ga}_2\text{O}_3$ .

gradual increase in the intensity of the lines due to both anatase and gallium oxide can be noted. In a related study, Rozdin and co-workers<sup>23</sup> reported the formation of three different gallium titanates: metatitanate ( $\text{Ga}_2\text{O}_3\cdot\text{TiO}_2$ ), dititanate ( $\text{Ga}_2\text{O}_3\cdot 2\text{TiO}_2$ ), and a tritanate with high  $\text{TiO}_2$  content (containing  $>90$  mol %  $\text{TiO}_2$ ) and designed as the  $\delta$ -phase. Further, they also found that there is no formation of a solid solution between  $\text{TiO}_2$  and  $\text{Ga}_2\text{O}_3$ , except at 1473 K, where a formation of  $\text{Ga}_2\text{O}_3$  in  $\text{TiO}_2$  with  $<1$  mol % is noted. The Ga metatitanate does not have a homogeneity region. The Ga dititanate is metastable at normal temperatures and is stable only at temperatures  $>1773$  K; its melting point is 1953 K. The homogeneity of the third titanate is 2.5%. The  $\text{Ga}_2\text{O}_3\text{-TiO}_2$  mixed oxide obtained from the homogeneous coprecipitation method in the present study appears to be a mixture of both component oxides. Very interestingly, no diffraction lines due to the rutile phase are observed. Thus, the  $\text{Ga}_2\text{O}_3\text{-TiO}_2$  mixed oxide contains mainly the anatase phase of titania and the  $\alpha$ -phase of gallia, which is quite stable up to a calcination temperature of 1073 K.

The XRD profiles of the 4 wt %  $\text{V}_2\text{O}_5/\text{Ga}_2\text{O}_3\text{-TiO}_2$  catalyst calcined at different temperatures is shown in Figure 5. As can be noted from this figure, the  $\text{V}_2\text{O}_5/\text{Ga}_2\text{O}_3\text{-TiO}_2$  calcined at 773 K exhibits broad but well-defined XRD lines due to anatase and  $\alpha\text{-Ga}_2\text{O}_3$ . On increasing calcination temperature from 773 to 873 K a further improvement in the intensity of the lines due to anatase and  $\alpha\text{-Ga}_2\text{O}_3$  can be noted. In addition, a few weak new peaks at  $d = 2.816$ ,  $2.547$ , and  $2.924$  Å can also be noted. The new lines were attributed to the presence of  $\beta\text{-Ga}_2\text{O}_3$  (JCPDS Files No. 11-370) phase. Upon a further increase of calcination to 973 K a partial transformation of titania anatase into rutile ( $\sim 60\%$ ) and total transformation of  $\alpha$ -gallia to  $\beta$ -gallia phase is noted. On further increase of calcination temperature to 1073 K a further increase in the intensity of the lines due to rutile and  $\beta$ -gallia can be noted. However, the transformation

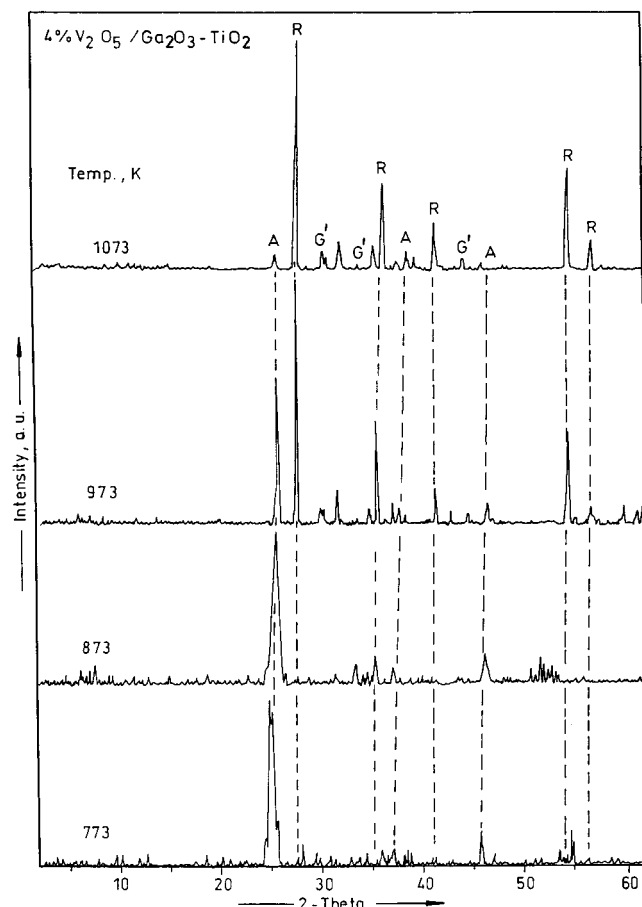


**Figure 5.** X-ray powder diffraction patterns of  $\text{Ga}_2\text{O}_3\text{-TiO}_2$  calcined at different temperatures: (A) lines due to anatase; (G') lines due to  $\beta\text{-Ga}_2\text{O}_3$ .

of anatase to rutile is not total even after calcination at 1073 K. This is an important observation in this study. Another important point to be noted from Figure 4 is that there are no lines either due to  $\text{V}_2\text{O}_5$  or to a compound between vanadia and gallia-titania even up to the calcination of 1073 K. The XRD results thus indicate that vanadium oxide is either in a highly dispersed state or the crystallites formed are less than the detection capability of the XRD technique. In the case of  $\text{V}_2\text{O}_5/\text{TiO}_2$  catalysts, reduction of some of the dispersed vanadia into the titania framework forming a rutile solid solution at 1073 K is an established fact in the literature.<sup>2,32-34</sup> It is also well-known in the literature that for vanadia contents of less than monolayer coverage, the active component will be present as a two-dimensional vanadium oxide overlayer on the support surface. Quantities in excess of monolayer coverage will have microcrystalline  $\text{V}_2\text{O}_5$  particles in addition to the surface vanadium oxide overlayer.<sup>2,3</sup> Rozdin and co-workers<sup>23</sup> further reported that there is no compound formation between  $\text{Ga}_2\text{O}_3$  and  $\text{V}_2\text{O}_5$  at 947–1173 K for 6–250 h of heating and having 1:3, 1:1, and 3:1 molar ratios; however,  $\alpha\text{-Ga}_2\text{O}_3$  was transformed to  $\beta\text{-Ga}_2\text{O}_3$ . The present XRD results also reveal that there is no compound formation between  $\text{V}_2\text{O}_5$  and  $\text{Ga}_2\text{O}_3$  up to a calcination of 1073 K and coincides with the earlier reports in the literature. A closer look at the XRD patterns of  $\text{TiO}_2$ ,  $\text{Ga}_2\text{O}_3\text{-TiO}_2$ ,  $\text{V}_2\text{O}_5/\text{TiO}_2$ , and  $\text{V}_2\text{O}_5/\text{Ga}_2\text{O}_3\text{-TiO}_2$  samples calcined at various temperatures (Figures 2–5) reveals that the  $\text{Ga}_2\text{O}_3$  in the  $\text{V}_2\text{O}_5/\text{TiO}_2$  catalyst exhibits a different behavior when compared to  $\text{TiO}_2$  alone. An interesting observation to be noted from these figures is that the 4%  $\text{V}_2\text{O}_5/\text{Ga}_2\text{O}_3\text{-TiO}_2$  sample contains some ( $<5\%$ ) anatase phase even after calcination at

**TABLE 1: Influence of Calcination Temperature on TiO<sub>2</sub> Phase Modification and Its Crystallite Size in V<sub>2</sub>O<sub>5</sub>/TiO<sub>2</sub> and V<sub>2</sub>O<sub>5</sub>/Ga<sub>2</sub>O<sub>3</sub>–TiO<sub>2</sub> Samples and the Corresponding Supports<sup>a</sup>**

<i>T</i> (K)	TiO <sub>2</sub> (nm)		V <sub>2</sub> O <sub>5</sub> /TiO <sub>2</sub> (nm)		Ga <sub>2</sub> O <sub>3</sub> –TiO <sub>2</sub> (nm)		V <sub>2</sub> O <sub>5</sub> /Ga <sub>2</sub> O <sub>3</sub> –TiO <sub>2</sub> (nm)	
	A	R	A	R	A	R	A	R
773	12.6		36.4		6.1		9.8	
873	nd	nd	44.0		7.1		15.8	
973	nd	nd	46.1	47.6	12.9		18.2	19.1
1073	22.4			54.5	19.6		17.0	19.1

<sup>a</sup> The (101) plane of anatase (A) and (110) plane of rutile (R) was considered for crystallite size measurements. nd, not done.

1073 K unlike the V<sub>2</sub>O<sub>5</sub>/TiO<sub>2</sub> sample. The vanadia in V<sub>2</sub>O<sub>5</sub>/TiO<sub>2</sub> or V<sub>2</sub>O<sub>5</sub>/Ga<sub>2</sub>O<sub>3</sub>–TiO<sub>2</sub> catalysts accelerates the transformation of anatase to rutile and α-gallia to β-gallia. On the other hand, the presence of gallia retards the transformation of anatase to rutile in the V<sub>2</sub>O<sub>5</sub>/Ga<sub>2</sub>O<sub>3</sub>–TiO<sub>2</sub> sample.

To understand the influence of gallium oxide on crystallite growth, the crystallite size of anatase and rutile in various samples was estimated from XRD measurements and shown in Table 1. The TiO<sub>2</sub> and Ga<sub>2</sub>O<sub>3</sub>–TiO<sub>2</sub> mixed oxide support contains only the anatase phase, whose crystallite size was found to increase with increasing calcination temperature. In the case of V<sub>2</sub>O<sub>5</sub>-containing catalysts both anatase and rutile phases are present. The crystallite size of both anatase and rutile in V<sub>2</sub>O<sub>5</sub>/TiO<sub>2</sub> are found to be larger than that in the V<sub>2</sub>O<sub>5</sub>/Ga<sub>2</sub>O<sub>3</sub>–TiO<sub>2</sub> sample. The scanning electron microscopy study of these samples also confirmed these observations. The results presented in Table 1 clearly indicate that the Ga<sub>2</sub>O<sub>3</sub> in V<sub>2</sub>O<sub>5</sub>/TiO<sub>2</sub> is retarding the phase transformation as well as grain growth of titania. It is a general phenomenon in catalysis that the catalysts with smaller particle size exhibit more specific surface area and better catalytic properties. In fact, the gallia–titania-supported vanadia was found to exhibit better activity and selectivity for the oxidation of 4-methylanisole to anisaldehyde<sup>21</sup> and one-step synthesis of 2,6-dimethylphenol from methanol and cyclohexanone mixtures.<sup>22</sup> The high specific surface area and smaller crystallite size may perhaps be the reason for the observed better catalytic properties, apart from the acid–base and redox characteristics of this complex catalyst.

The infrared spectroscopy has been widely used to ascertain the nature of vanadium oxide phase on various supports.<sup>2,3</sup> The FTIR spectra of Ga<sub>2</sub>O<sub>3</sub>–TiO<sub>2</sub>, 4% V<sub>2</sub>O<sub>5</sub>/TiO<sub>2</sub>, and 4% V<sub>2</sub>O<sub>5</sub>/Ga<sub>2</sub>O<sub>3</sub>–TiO<sub>2</sub> samples calcined at different temperatures are included in the Supporting Information (Figures 1S, 2S, and 3S, respectively). These spectra were recorded in the range 400–1200 cm<sup>−1</sup>, where those bands due to the ν<sub>V=O</sub> are expected to be observed. The FTIR spectra of Ga<sub>2</sub>O<sub>3</sub> (commercial sample) and TiO<sub>2</sub> anatase (commercial sample) are also recorded in the same range, for the purpose of better comparison, and are shown in these figures. Titania anatase exhibits strong absorption bands at 676 and 547 cm<sup>−1</sup>, and the rutile has bands at 660 and 455 cm<sup>−1</sup>, respectively.<sup>35</sup> As presented in Figure 1S, the pure Ga<sub>2</sub>O<sub>3</sub> oxide exhibits strong absorption bands at 680–720 and 460–500 cm<sup>−1</sup> and the pure titania anatase has bands at 550–670 cm<sup>−1</sup>. However, the Ga<sub>2</sub>O<sub>3</sub>–TiO<sub>2</sub> binary oxide support did not exhibit any sharp absorption bands up to the calcination temperature of 973 K, but at 1073 K some broad bands in the region between 550 and 750 cm<sup>−1</sup> were observed. It is an established fact in the literature<sup>2,36</sup> that the IR spectrum of pure V<sub>2</sub>O<sub>5</sub> shows sharp absorption bands at 1020 cm<sup>−1</sup> and another at 820 cm<sup>−1</sup> due to V=O stretching and V–O–V deformation modes, respectively. As presented in Figures 2S and 3S, the

**TABLE 2: Influence of Calcination Temperature on the BET Surface Area, O<sub>2</sub> Chemisorption, and Dispersion of Vanadium**

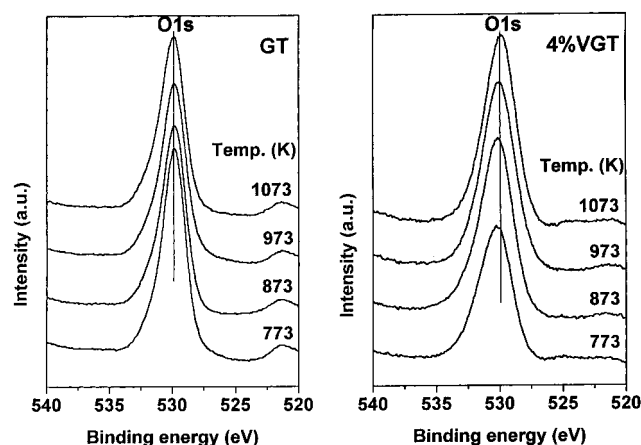
sample	BET SA (m <sup>2</sup> g <sup>−1</sup> )	O <sub>2</sub> uptake (μmol g <sup>−1</sup> catalyst)	% dispersion (O/V)
773 K			
Ga <sub>2</sub> O <sub>3</sub> –TiO <sub>2</sub>	122	2.9	
V <sub>2</sub> O <sub>5</sub> /Ga <sub>2</sub> O <sub>3</sub> –TiO <sub>2</sub>	96	159	72
873 K			
Ga <sub>2</sub> O <sub>3</sub> –TiO <sub>2</sub>	96		
V <sub>2</sub> O <sub>5</sub> /Ga <sub>2</sub> O <sub>3</sub> –TiO <sub>2</sub>	77	149	68
973 K			
Ga <sub>2</sub> O <sub>3</sub> –TiO <sub>2</sub>	73		
V <sub>2</sub> O <sub>5</sub> /Ga <sub>2</sub> O <sub>3</sub> –TiO <sub>2</sub>	22	132	62
1073 K			
Ga <sub>2</sub> O <sub>3</sub> –TiO <sub>2</sub>	51		
V <sub>2</sub> O <sub>5</sub> /Ga <sub>2</sub> O <sub>3</sub> –TiO <sub>2</sub>	7	112	51

spectra of V<sub>2</sub>O<sub>5</sub>/TiO<sub>2</sub> and V<sub>2</sub>O<sub>5</sub>/Ga<sub>2</sub>O<sub>3</sub>–TiO<sub>2</sub> catalysts calcined at 773 K did not reveal the presence of crystalline V<sub>2</sub>O<sub>5</sub>. These spectra are identical with that of pure supports, in agreement with the XRD observations, where only the anatase phase of TiO<sub>2</sub> is noted. However, with increasing calcination temperature from 773 to 1073 K a gradual transformation of anatase into rutile was also noted from IR results in line with XRD observations. In the case of the 4% V<sub>2</sub>O<sub>5</sub>/Ga<sub>2</sub>O<sub>3</sub>–TiO<sub>2</sub> sample calcined at 1073 K, a sharp absorption band in the region between 680 and 720 cm<sup>−1</sup> was also noted due to β-Ga<sub>2</sub>O<sub>3</sub> in agreement with the XRD observations. A weak band at around 980 cm<sup>−1</sup> was also noted in these spectra. This particular band, in the range 990–960 cm<sup>−1</sup>, has been reported frequently for vanadia–titania catalysts having the vanadium content close to that necessary to cover the support surface with a single “monolayer”.<sup>2,36</sup> Incidentally, the V<sub>2</sub>O<sub>5</sub> content present in the sample corresponds to less than monolayer capacity of the Ga<sub>2</sub>O<sub>3</sub>–TiO<sub>2</sub> support.<sup>2</sup> Thus, the FTIR results also suggest that the impregnated vanadium oxide is in a highly dispersed state on the support surface, especially at 773 K calcination temperature, coinciding with the XRD results. These observations were further confirmed from O<sub>2</sub> uptake measurements as described in the following paragraphs.

The BET surface area, oxygen uptake capacity, and dispersion of vanadium oxide on Ga<sub>2</sub>O<sub>3</sub>–TiO<sub>2</sub> support as a function of calcination temperature are shown in Table 2. A considerable decrease in the specific surface area of the samples with increasing calcination temperature can be noted from this table. The decrease in specific surface area with increase in calcination temperature is a general phenomenon and is expected to be due to sintering of the samples at higher temperatures. Another interesting point to be noted from this table is that the decrease of specific surface area is more in the case of vanadia-impregnated catalysts than that of pure support. This observation once again indicates that the gallia–titania mixed oxide is quite thermally stable when compared to that of vanadia-impregnated samples. The BET surface area of the commercial TiO<sub>2</sub> sample was 10 m<sup>2</sup> g<sup>−1</sup> and decreased to 6 m<sup>2</sup> g<sup>−1</sup> after impregnation with V<sub>2</sub>O<sub>5</sub>. The surface areas of both TiO<sub>2</sub> and V<sub>2</sub>O<sub>5</sub>/TiO<sub>2</sub> decreased to less than unity with increasing calcination temperature beyond 873 K. The O<sub>2</sub> uptake capacity of the V<sub>2</sub>O<sub>5</sub>/TiO<sub>2</sub> was also found to be poor in view of its low specific surface area. Oxygen uptakes at 643 K on the prereduced V<sub>2</sub>O<sub>5</sub>/Ga<sub>2</sub>O<sub>3</sub>–TiO<sub>2</sub> catalyst, calcined at different temperatures is shown in Table 2. The pure Ga<sub>2</sub>O<sub>3</sub>–TiO<sub>2</sub> support was also found to chemisorb some small amount of O<sub>2</sub> under experimental conditions employed in this study. Therefore, the contribution

**TABLE 3: XPS Binding Energies, Kinetic Energies, Atomic Intensity Ratios, and Auger Parameter Values of Ga<sub>2</sub>O<sub>3</sub>–TiO<sub>2</sub> Support and V<sub>2</sub>O<sub>5</sub>/Ga<sub>2</sub>O<sub>3</sub>–TiO<sub>2</sub> Catalyst Calcined at Different Temperatures**

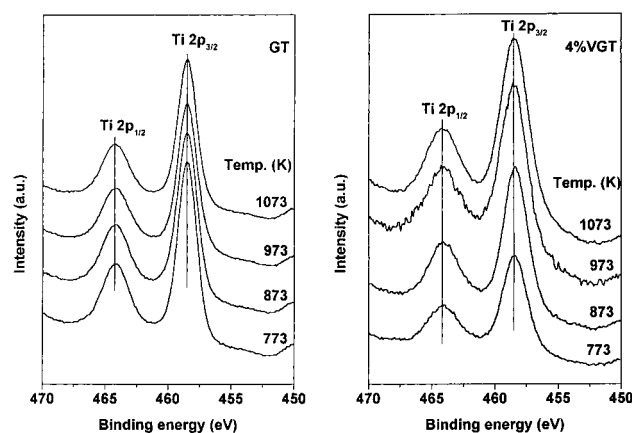
T (K)	Ti 2p <sub>3/2</sub>	Ti KE	α' Ti	Ga 3d	Ga KE	α' Ga	O 1s	V 2p <sub>3/2</sub>	Ti/Ga	V/Ti	V/Ga
Ga <sub>2</sub> O <sub>3</sub> –TiO <sub>2</sub>											
773	458.5	414.5	873.0	20.4	1063.4	1083.8	529.9		1.51		
873	458.5	414.5	873.0	20.0	1063.4	1083.4	529.8		1.32		
973	458.5	414.6	873.1	19.7	1063.5	1083.2	529.9		1.21		
1073	458.5	414.4	872.9	19.5	1063.6	1083.1	529.9		1.14		
V <sub>2</sub> O <sub>5</sub> /Ga <sub>2</sub> O <sub>3</sub> –TiO <sub>2</sub>											
773	458.5	414.8	873.3	19.9	1063.2	1083.1	530.2	517.3	0.59	0.46	0.27
873	458.5	414.7	873.2	20.0	1063.2	1083.2	530.1	517.1	0.69	0.39	0.27
973	458.5	414.6	873.1	20.2	1063.3	1083.5	530.0	517.0	0.99	0.15	0.15
1073	458.5	414.5	873.0	20.4	1063.1	1083.6	529.9	516.8	1.11	0.09	0.10

**Figure 6.** O 1s XPS spectra of Ga<sub>2</sub>O<sub>3</sub>–TiO<sub>2</sub> and 4% V<sub>2</sub>O<sub>5</sub>/Ga<sub>2</sub>O<sub>3</sub>–TiO<sub>2</sub> samples calcined at different temperatures.

of pure support alone was subtracted from the results. Increasing the calcination temperature apparently results in a decrease in the dispersion of V<sub>2</sub>O<sub>5</sub>, especially in the case of catalysts calcined at 1073 K. However, for the sample calcined at 773 K the dispersion remains high. The O<sub>2</sub> chemisorption is possible only on the reduced V-oxide, which contains the coordinately unsaturated sites. This method thus, discriminates between the monolayer and crystalline V-oxide phases since their reduction behaviors are entirely different.<sup>12,27,37,38</sup> The decrease in the dispersion with increase in calcination temperature is primarily due to sintering of the samples at higher calcination temperatures and subsequent phase transformation of titania anatase into rutile and α-gallia into β-gallia. Thus, O<sub>2</sub> uptake results are in line with XRD and FTIR observations.

The samples of Ga<sub>2</sub>O<sub>3</sub>–TiO<sub>2</sub> and 4% V<sub>2</sub>O<sub>5</sub>/Ga<sub>2</sub>O<sub>3</sub>–TiO<sub>2</sub> calcined at different temperatures are investigated by XPS technique. The photoelectron peaks of O 1s, Ti 2p, Ga 3d, and V 2p are depicted in Figures 6–9, respectively. For the purpose of better comparison, the XPS photoelectron peaks of O 1s, Ti 2p, and Ga 3d pertaining to Ga<sub>2</sub>O<sub>3</sub>–TiO<sub>2</sub> carrier and the corresponding peaks of the V<sub>2</sub>O<sub>5</sub>/Ga<sub>2</sub>O<sub>3</sub>–TiO<sub>2</sub> catalyst are presented together in these figures. Binding energies for O 1s, Ti 2p, Ga 3d, and V 2p core levels, and the Auger parameters of Ti 2p and Ga 3d along with kinetic energies of Ti and Ga are shown in Table 3. The Ti/Ga, V/Ti, and V/Ga atomic ratios as determined by XPS are shown in Figure 10 and Table 3. All these figures and Table 3 clearly indicate that the XPS bands depend on calcination temperature and the coverage of vanadium oxide on the carrier, in agreement with the literature reports.<sup>39–43</sup>

The O 1s profile, as shown in Figure 6, is due to the overlapping contribution of oxygen from gallia and titania in the case of Ga<sub>2</sub>O<sub>3</sub>–TiO<sub>2</sub> support and gallia, titania, and vanadia in the case of the V<sub>2</sub>O<sub>5</sub>/Ga<sub>2</sub>O<sub>3</sub>–TiO<sub>2</sub> catalyst, respectively. The

**Figure 7.** Ti 2p XPS spectra of Ga<sub>2</sub>O<sub>3</sub>–TiO<sub>2</sub> and 4% V<sub>2</sub>O<sub>5</sub>/Ga<sub>2</sub>O<sub>3</sub>–TiO<sub>2</sub> samples calcined at different temperatures.

binding energy of the most intense O 1s peak (Table 3), in the case of Ga<sub>2</sub>O<sub>3</sub>–TiO<sub>2</sub> sample, is almost constant with increasing calcination temperature. However, a slight shift at higher binding energies can be noted in the case of the V<sub>2</sub>O<sub>5</sub>/Ga<sub>2</sub>O<sub>3</sub>–TiO<sub>2</sub> sample calcined at 973–773 K. A clear broadening of the peak after impregnating with vanadia can also be noted from Figure 6 due to a strong interaction between the vanadia and gallia portion of the gallia–titania mixed oxide, more details of which are given in later paragraphs. Another interesting point to be noted from Figure 6 is that the intensity of the O 1s of the Ga<sub>2</sub>O<sub>3</sub>–TiO<sub>2</sub> sample decreases very slightly with increasing calcination temperature whereas in the case of the V<sub>2</sub>O<sub>5</sub>/Ga<sub>2</sub>O<sub>3</sub>–TiO<sub>2</sub> sample it increases. A similar intensity variation in the Ti 2p lines of Ga<sub>2</sub>O<sub>3</sub>–TiO<sub>2</sub> and V<sub>2</sub>O<sub>5</sub>/Ga<sub>2</sub>O<sub>3</sub>–TiO<sub>2</sub> samples can also be noted (Figure 7). This is primarily due to crystallization of TiO<sub>2</sub> in Ga<sub>2</sub>O<sub>3</sub>–TiO<sub>2</sub> and V<sub>2</sub>O<sub>5</sub>/Ga<sub>2</sub>O<sub>3</sub>–TiO<sub>2</sub> samples, which increases with increasing calcination temperature. The maximum contributor for O 1s in Ga<sub>2</sub>O<sub>3</sub>–TiO<sub>2</sub> and V<sub>2</sub>O<sub>5</sub>/Ga<sub>2</sub>O<sub>3</sub>–TiO<sub>2</sub> samples is TiO<sub>2</sub> since its concentration is higher than those of other constituents.

Figure 7 shows the binding energies of Ti 2p photoelectron peaks at 458.5 and 464.4 eV for Ti 2p<sub>3/2</sub> and Ti 2p<sub>1/2</sub> lines, respectively, which agree well with the values reported in the literature.<sup>39,40,44,45</sup> Very interestingly, the intensity of the Ti 2p core level spectra increased with increasing calcination temperature. This increase is more prominent in the case of V<sub>2</sub>O<sub>5</sub>/Ga<sub>2</sub>O<sub>3</sub>–TiO<sub>2</sub> than Ga<sub>2</sub>O<sub>3</sub>–TiO<sub>2</sub>, indicating that the intensity of Ti 2p photoelectron signals depends on the calcination temperature as well as on the coverage of V<sub>2</sub>O<sub>5</sub> on the gallia–titania carrier. The Auger parameter for Ti has been measured and summarized in Table 3, showing very small but insignificant variation for both gallia–titania and vanadia-doped gallia–titania catalysts. As this parameter does not depend on charge effects, the Ti seems to be in a similar chemical state for all the



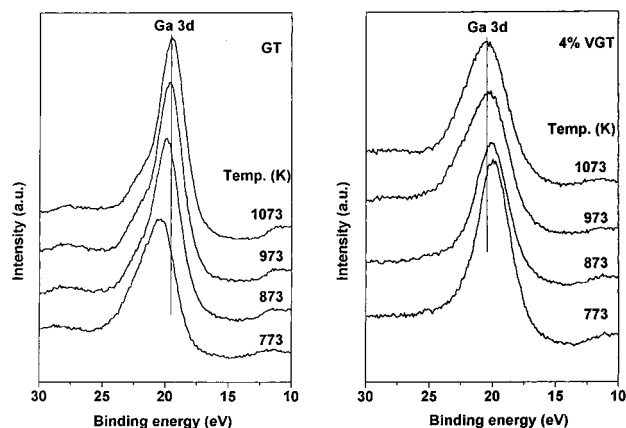


**Figure 8.** Ga 3d XPS spectra of  $\text{Ga}_2\text{O}_3\text{--TiO}_2$  and 4%  $\text{V}_2\text{O}_5/\text{Ga}_2\text{O}_3\text{--TiO}_2$  samples calcined at different temperatures.

samples. Therefore, Ti was considered as a good reference for binding energy calibrations.

Figure 8 and Table 3 show the binding energy, and the Auger parameter values of the Ga 3d core level spectra, which agree with the values reported in the literature.<sup>46</sup> It can be noted from this table that the core level binding energy increased with increasing calcination temperature in the case of the  $\text{V}_2\text{O}_5/\text{Ga}_2\text{O}_3\text{--TiO}_2$  sample. However, a decreasing trend was observed in the case of the  $\text{Ga}_2\text{O}_3\text{--TiO}_2$  support. Very interestingly, the intensity of the Ga 3d line increased with increasing calcination temperature in the case of the  $\text{Ga}_2\text{O}_3\text{--TiO}_2$  sample and decreased in the case of the  $\text{V}_2\text{O}_5/\text{Ga}_2\text{O}_3\text{--TiO}_2$  sample. The Auger parameter for Ga has been measured and summarized in Table 3, showing a significant variation for both gallia–titania and vanadia/gallia–titania samples. Decrease in binding energy with increase in the calcination temperature, in the case of pure gallia–titania, suggests that the  $\text{Ga}_2\text{O}_3$  is partially reduced. However, an opposite trend was observed in the case of vanadia-doped  $\text{Ga}_2\text{O}_3\text{--TiO}_2$  catalysts. The partial reduction in the case of  $\text{Ga}_2\text{O}_3\text{--TiO}_2$  may presumably be due to desorption of some loosely bound surface oxygen atoms at higher calcination temperatures. In the case of the  $\text{V}_2\text{O}_5/\text{Ga}_2\text{O}_3\text{--TiO}_2$  catalyst, while being subjected to higher calcination temperatures, the vanadia is found to reduce partially (Table 3, V 2p binding energy decreased). The partial reduction of vanadia in the case of the vanadia/gallia–titania catalyst indicates that vanadia is probably transforming from the octahedral to the tetrahedral state and stabilizing in the later state.<sup>2</sup> This stabilization may be due to an interaction between acidic vanadia and basic gallia. However, no formation of compound is identified from the XRD study. Diffusion of some of the vanadia into the bulk of the  $\text{Ga}_2\text{O}_3\text{--TiO}_2$  mixed oxide at higher calcination temperatures can also be expected.

Figure 9 shows the V  $2p_{3/2}$  photoelectron peak of the  $\text{V}_2\text{O}_5/\text{Ga}_2\text{O}_3\text{--TiO}_2$  sample calcined at various temperatures. A significant decrease in the intensity and extensive broadening of the V 2p line can be noted with increasing calcination temperature. The broadening of the XPS peak can be attributed to various factors including (1) the presence of more than one type of  $\text{V}^{5+}$  with different chemical characteristics, which cannot be discerned by ESCA, and (2) electron transfer between the active component and the support (metal–support interaction). At 773 K calcination the binding energy of  $\text{V}2p_{3/2}$  is 517.3 eV; it probably corresponds to the  $\text{V}^{5+}$  state. With increasing calcination temperature from 773 to 1073 K, the binding energy of V  $2p_{3/2}$  decreased from 517.3 to 516.8 eV (Table 3). A careful examination of literature reveals that the V  $2p_{3/2}$  binding energy

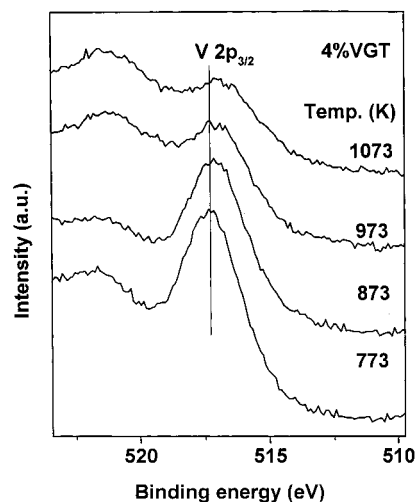


**Figure 9.** V 2p XPS spectra of 4%  $\text{V}_2\text{O}_5/\text{Ga}_2\text{O}_3\text{--TiO}_2$  sample calcined at different temperatures.

reported for  $\text{V}_2\text{O}_5$  ( $\text{V}^{5+}$  oxidation state) ranges between 517.4 and 516.4 eV; the next oxidation,  $\text{V}^{4+}$ , represented by  $\text{V}_2\text{O}_4$ , shows values in the range 515.7–515.4 eV.<sup>2,47–49</sup> The decrease in binding energy with increasing calcination temperature indicates that a part of vanadium oxide is stabilized in a lower oxidation (tetravalent) state at higher calcination temperatures. This may be due to either the formation of a solid solution between vanadia–titania (known in the literature) or vanadia–gallia (not well established) or a diffusion of vanadium oxide into the bulk of gallia–titania. It appears that vanadia in the pentavalent state is stabilized on the  $\text{Ga}_2\text{O}_3\text{--TiO}_2$  mixed oxide support when calcined at 773 K. As the calcination temperature increases, the transformation of gallia from  $\alpha$ - to  $\beta$ -phase and titania from anatase to rutile occurs, thereby increasing the interparticle distances between the oxide components, leading to the diffusion of some of the vanadia into the bulk. Thus, diffused vanadia may be stabilized in the tetravalent state by interacting with the newly formed oxides of the carrier. As mentioned earlier, in the case of the  $\text{V}_2\text{O}_5/\text{Ga}_2\text{O}_3\text{--TiO}_2$  sample, the intensity of the Ga 3d line has decreased at the same time the binding energy has slightly increased with increasing calcination temperature. An exactly opposite trend is noted in the case of the  $\text{Ga}_2\text{O}_3\text{--TiO}_2$  sample, which indicates that gallium is partially reduced in the case of pure support due to loss of loosely bound oxygen and oxidized back in the case of the vanadia-containing sample at the expense of vanadia reduction. Very interestingly, such an effect is not observed in the case of Ti 2p spectra. This clearly indicates that with treatment at high temperatures the vanadia is preferentially interacting with the gallia component of the mixed oxide and not with titania. This mutual interaction may be the reason for the partial reduction of vanadia and partial oxidation of gallia in the  $\text{V}_2\text{O}_5/\text{Ga}_2\text{O}_3\text{--TiO}_2$  catalyst at higher temperatures.

The Ti/Ga atomic ratios, as determined by XPS, for both the  $\text{Ga}_2\text{O}_3\text{--TiO}_2$  support and  $\text{V}_2\text{O}_5/\text{Ga}_2\text{O}_3\text{--TiO}_2$  catalyst are shown in Figure 10a and Table 3. As can be noted from Table 3, the Ti/Ga atomic ratio is higher for the pure support than for the corresponding vanadia-impregnated samples, which indicates that the support surface is covered by a vanadium oxide monolayer. As can be noted from Figure 10a, the Ti/Ga atomic ratio has been decreased, in the case of pure support, with increasing calcination temperature. An opposite phenomenon is noted in the case of the  $\text{V}_2\text{O}_5/\text{Ga}_2\text{O}_3\text{--TiO}_2$  sample. A high Ti/Ga ratio at 773 K, in the case of  $\text{Ga}_2\text{O}_3\text{--TiO}_2$ , indicates that the surface is enriched with titania since the  $\text{TiO}_2$  to  $\text{Ga}_2\text{O}_3$  ratio

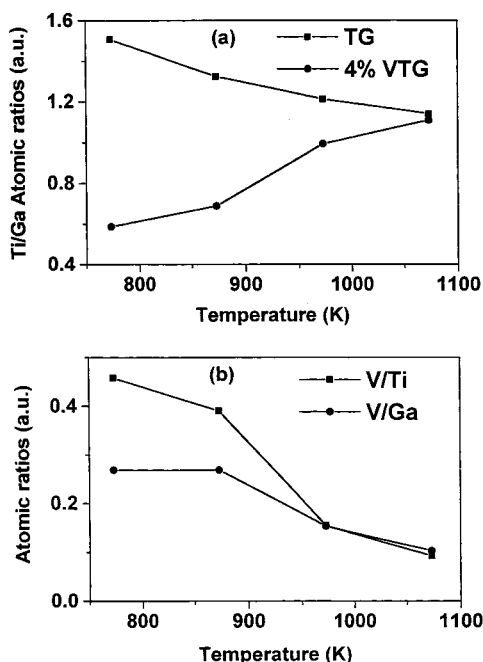


**Figure 10.** XPS atomic percentage ratios of  $\text{Ga}_2\text{O}_3\text{--TiO}_2$  and  $\text{V}_2\text{O}_5/\text{Ga}_2\text{O}_3\text{--TiO}_2$  samples at different temperatures.

in the mixed oxide is 5:1. However, as the calcination temperature increases, the composition near the surface region of the samples, both cases, has changed significantly. A redistribution of the component oxides is possible due to differences in their physical (such as density, Tamann temperature, etc.) and chemical (acid–base attraction, especially between vanadia and gallia) properties.<sup>50</sup> The support's surface is being enriched with gallia in the case of gallia–titania with the increase of temperature. However, in the case of the  $\text{V}_2\text{O}_5/\text{Ga}_2\text{O}_3\text{--TiO}_2$  catalyst, the surface is enriched with titania by increasing the temperature. From XRD study, the phase transformation of titania anatase to rutile was observed in the case of the  $\text{V}_2\text{O}_5/\text{Ga}_2\text{O}_3\text{--TiO}_2$  catalyst (Figure 4) with increasing calcination temperature. Besides the phase transformation, the crystalline size of titania was also increased significantly (Table 2). With an increase in the crystalline size of titania, the surface is becoming enriched with  $\text{TiO}_2$ . This may be the reason for an increase in the Ti/Ga ratio with increasing calcination temperature as well as the intensity of the Ti  $2p_{3/2}$  peak for the  $\text{V}_2\text{O}_5/\text{Ga}_2\text{O}_3\text{--TiO}_2$  catalyst, as observed in Figure 7.

The relative dispersion of vanadium oxide on the support surface was also estimated from XPS measurements of the  $\text{V}_2\text{O}_5/\text{Ga}_2\text{O}_3\text{--TiO}_2$  catalyst calcined at different temperatures and presented in Table 3 and Figure 10b. The intense signal corresponding to the V  $2p_{3/2}$  level of vanadium was compared with the Ti  $2p_{3/2}$  and Ga 3d levels. The V  $2p/\text{Ti } 2p$  and V  $2p/\text{Ga } 3d$  atomic ratios can be taken as a measure of relative dispersion of vanadium oxide on the support surface. In general, the V/Ti and V/Ga ratios are found to decrease with increasing calcination temperature. The difference between V/Ti and V/Ga ratios also decreased with increasing calcination temperature and are almost the same at 973 and 1073 K. The decrease in V/Ti and V/Ga ratios with increasing calcination temperature is primarily due to segregation of dispersed vanadium oxide into the bulk of the support. As shown in Table 2, with an increase of calcination temperature a decrease in the specific surface area of the samples thereby decreasing the proportion of dispersed vanadium oxide on the surface has been observed. Under the influence of thermal treatments, the dispersed vanadia

agglomerates into microcrystalline vanadium oxide particles and diffuses into the bulk. During this process a part of vanadia may be incorporated into the gallium oxide structure. The XRD results clearly showed the influence of vanadia on the transformation of  $\alpha\text{-Ga}_2\text{O}_3$  into  $\beta\text{-Ga}_2\text{O}_3$  at higher temperatures. The XPS measurements also reveal an extensive broadening of both Ga 3d and V  $2p_{3/2}$  lines with increasing calcination temperature. On the other hand the intensity of the Ti 2p line was found to increase with increasing calcination temperature. It is an established fact in the literature that dispersed vanadia on the  $\text{TiO}_2$  surface accelerates the phase transformation. In fact, the present investigation also established beyond a doubt the influence of vanadia on the phase transformation of anatase into rutile (Figures 2 and 3). As reported in the literature, during this phase transformation some of the dispersed  $\text{V}_2\text{O}_5$  normally is reduced and gets incorporated into the rutile structure as  $\text{V}_x\text{Ti}_{(1-x)}\text{O}_2$  (rutile solid solution).<sup>2,32–33</sup> However, the present XPS measurements provide an impression that the dispersed vanadia interacts preferably with gallia instead of titania in the mixed oxide matrix. However, no definite compounds between vanadia and gallia are observed from the XRD study. Nevertheless, the combined  $\text{V}_2\text{O}_5/\text{Ga}_2\text{O}_3\text{--TiO}_2$  mixed oxide catalyst exhibits very interesting catalytic properties.<sup>21,22</sup>

## Conclusions

The following conclusions can be drawn from this study: (1) The  $\text{Ga}_2\text{O}_3\text{--TiO}_2$  mixed oxide obtained by a homogeneous coprecipitation method exhibits reasonably high specific surface area and high thermal stability up to 1073 K. It primarily consists of a mixture of anatase and  $\alpha\text{-Ga}_2\text{O}_3$ . (2) The gallia–titania mixed oxide is an interesting and promising support for the dispersion of vanadium oxide. Characterization of the  $\text{V}_2\text{O}_5/\text{Ga}_2\text{O}_3\text{--TiO}_2$  catalyst by XRD, FTIR, XPS, and  $\text{O}_2$  chemisorption revealed that the catalyst with 4 wt %  $\text{V}_2\text{O}_5$  consisted of a surface amorphous vanadium oxide phase dispersed on the carrier. When these catalysts were subjected to thermal treatments from 773 to 1073 K a gradual transformation of anatase to rutile and  $\alpha\text{-Ga}_2\text{O}_3$  to  $\beta\text{-Ga}_2\text{O}_3$  is noted. This transformation phenomenon is strongly promoted by vanadia and is accompanied by a loss in the specific surface area of the catalysts. In particular, the gallia in  $\text{V}_2\text{O}_5/\text{Ga}_2\text{O}_3\text{--TiO}_2$  catalysts retards the transformation of anatase to rutile under the influence of vanadia. (3) The XPS measurements further suggest that the dispersed vanadia interacts preferably with the gallia portion of the  $\text{Ga}_2\text{O}_3\text{--TiO}_2$  mixed oxide. However, the characterization results did not provide evidence about the formation of any specific compound between vanadia and gallia. (4) The  $\text{V}_2\text{O}_5/\text{Ga}_2\text{O}_3\text{--TiO}_2$  combination is an interesting catalyst possessing acid–base properties together with redox characteristics and highly promising for selective oxidation reactions.

**Acknowledgment.** E.P.R. thanks the Dirección General de Investigación Científica y Técnica (Spain) for financial support in the form of an International Postdoctoral Fellowship. I.G. is the recipient of Senior Research Fellowship of the University Grants Commission, New Delhi.

**Supporting Information Available:** FTIR spectra of  $\text{Ga}_2\text{O}_3\text{--TiO}_2$ , 4%  $\text{V}_2\text{O}_5/\text{TiO}_2$ , and 4%  $\text{V}_2\text{O}_5/\text{Ga}_2\text{O}_3\text{--TiO}_2$  samples calcined at different temperatures between 773 and 1073 K and recorded in the range  $400\text{--}1200\text{ cm}^{-1}$  are shown in Figures 1S, 2S, and 3S, respectively. This material is available free of charge via the Internet at <http://pubs.acs.org>.

## References and Notes

- (1) Hadjiivanov, K. I.; Klissurski, D. G. *Chem. Soc. Rev.* **1996**, 25, 61 and references therein.
- (2) Bond, G. C.; Tahir, S. F. *Appl. Catal.* **1991**, 71, 1 and references therein.
- (3) Deo, G.; Wachs, I. E.; Haber, J. *Crit. Rev. Sci. Eng.* **1994**, 19, 141.
- (4) Anpo, M. *Res. Chem. Intermed.* **1989**, 11, 67.
- (5) Taramasso, M.; Perego, G.; Notari, B. U.S. Patent 4,410,501. 1983.
- (6) Kumar, K. N. P.; Keizer, K.; Burggraaf, A. J. *J. Mater. Sci. Lett.* **1994**, 13, 59.
- (7) LeDuc, C. A.; Campbell, J. M.; Rossin, J. A. *Ind. Eng. Chem. Res.* **1996**, 35, 2473.
- (8) Gopalan, R.; Lin, Y. S. *Ind. Eng. Chem. Res.* **1995**, 34, 1189.
- (9) Baiker, A.; Dollenmeier, P.; Glinski, M.; Reller, A. *Appl. Catal.* **1987**, 35, 351.
- (10) Reichmann, M. G.; Bell, A. T. *Appl. Catal.* **1987**, 32, 315.
- (11) Wauthoz, P.; Ruwet, M.; Machej, T.; Grange, P. *Appl. Catal.* **1991**, 69, 149.
- (12) Reddy, B. M.; Kumar, M. V.; Reddy, E. P.; Mehdi, S. *Catal. Lett.* **1996**, 36, 187.
- (13) Harle, V.; Vrinat, M.; Scharff, J.-P.; Durand, B.; Deloume, J.-P. *Appl. Catal. A: General* **2000**, 196, 261.
- (14) Burford, S. N.; Davies, E. E. U.S. Patent 41, 573, 565. 1979.
- (15) Nakagawa, K.; Okamura, M.; Ikenaga, N.; Suzuki, T.; Kobayashi, T. *J. Chem. Soc., Chem. Commun.* **1998**, 1025.
- (16) Mowry, J. R.; Anderson, R. F.; Jonson, J. A. *J. Oil Gas* **1985**, 128.
- (17) Kitagawa, H.; Sendoda, Y.; Ono, Y. *J. Catal.* **1986**, 101, 12.
- (18) Gnep, G. N.; Doyemet, J. Y.; Seco, A. M.; Riebeiro, F. R.; Guisnet, M. *Appl. Catal.* **1988**, 43, 105.
- (19) Thomas, J. M.; Liu, X. *J. Phys. Chem.* **1986**, 90, 4843.
- (20) Gnep, N. S.; Doyemet, J. Y.; Guisnet, M. *J. Mol. Catal.* **1988**, 45, 281.
- (21) Reddy, B. M.; Ganesh, I.; Chowdhury, B. *Chem. Lett.* **1997**, 1145.
- (22) Reddy, B. M.; Ganesh, I. *J. Mol. Catal. A: Chem.* **2001**, 169, 207.
- (23) Rozdin, I. A.; Plotkin, S. S.; Plyushchev, V. E.; Sorokin, N. I. *Neorg. Mater.* **1975**, 11, 178.
- (24) Antsiferov, V. N.; Filimonova, I. V.; Makarov, A. M. *Russ. J. Appl. Chem.* **1999**, 72, 1019.
- (25) Reddy, B. M.; Manohar, B.; Mehdi, S. *J. Solid State Chem.* **1992**, 97, 233.
- (26) Klug, H. P.; Alexander, L. E. *X-ray Diffraction Procedures for Polycrystalline and Amorphous Materials*, 2nd ed.; John Wiley and Sons: New York, 1974.
- (27) Reddy, B. M.; Monohor, B.; Reddy, E. P. *Langmuir* **1993**, 9, 1781.
- (28) Briggs, D.; Seah, M. P., Eds. *Practical Surface Analysis*, 2nd ed.; Auger and X-ray Photoelectron Spectroscopy; Wiley: New York, 1990; Vol. 1.
- (29) Shirley, D. A. *Phys. Rev. B* **1972**, 5, 4709.
- (30) Savitzky, A.; Golay, M. J. E. *Anal. Chem.* **1964**, 36, 1627.
- (31) Lassaletta, G.; Fernández, A.; Espinós, J. P.; González-Elipe, A. R. *J. Phys. Chem.* **1995**, 99, 1484.
- (32) Kozłowski, R.; Pettifer, R. F.; Thomas, J. M. *J. Phys. Chem.* **1983**, 87, 5176.
- (33) Roozeboom, F.; Mittlemeijer-Hazeleger, M. C.; Moulin, J. A.; Medema, J.; de Beer, V. H.; Gellings, P. J. *J. Phys. Chem.* **1980**, 84, 2783.
- (34) Vejux, A.; Courtine, P. *J. Solid State Chem.* **1978**, 23, 93.
- (35) Nyquist, R. A.; Putzig, L. L.; Leugers, M. A. *Hand Book of Infrared and Raman Spectra of Inorganic Compounds and Organic Salts*; Academic Press: New York, 1997.
- (36) Nakagawa, Y.; Ono, J.; Miyata, H.; Kubokawa, Y. *J. Chem. Soc., Faraday Trans.* **1993**, 79, 2929.
- (37) Reddy, B. M.; Mehdi, S.; Reddy, E. P. *Catal. Lett.* **1993**, 20, 317.
- (38) Oyama, S. T.; Went, G. T.; Bell, A. T.; Somarjai, G. A. *J. Phys. Chem.* **1989**, 93, 6786.
- (39) Reddy, B. M.; Ganesh, I.; Reddy, E. P. *J. Phys. Chem. B* **1997**, 101, 1769.
- (40) Reddy, B. M.; Chowdhary, B.; Ganesh, I.; Reddy, E. P.; Rojas, T. C.; Fernández, A. *J. Phys. Chem. B* **1998**, 102, 10176.
- (41) Galan-Fereres, M.; Mariscal, R.; Alemany, L. J.; Fierro, J. L. G.; Anderson, J. A. *J. Chem. Soc., Faraday Trans.* **1994**, 90, 3711.
- (42) Nag, N. K.; Massoth, F. E. *J. Catal.* **1990**, 124, 127.
- (43) Jonson, B.; Robenstorff, B.; Larsson, R.; Andersson, S. L. T. *J. Chem. Soc., Faraday Trans.* **1988**, 84, 1897.
- (44) Gao, X.; Bare, S. R.; Fierro, J. L. G.; Banares, M. A.; Wachs, I. E. *J. Phys. Chem. B* **1998**, 102, 5653.
- (45) Sawatzky, G. A.; Post, D. *Phys. Rev.* **1979**, B20, 1546.
- (46) Iwakuro, H.; Tatsuyama, C.; Ichimura, S. *Jpn. J. Appl. Phys.* **1982**, 21, 94.
- (47) Rao, C. N. R.; Sarma, D. D.; Vasudevan, S.; Hedge, M. S. *Proc. R. Soc. London Ser. A* **1979**, 367, 239.
- (48) Nogier, J. Ph.; Delmer, M. *Catal. Today* **1994**, 20, 109.
- (49) Bukhtiyarov, V. I. *Catal. Today* **2000**, 56, 403.
- (50) Anderson, J. R. *Structure of Metallic Catalysts*; Academic Press: New York, 1975, p 62.